Table S1. Primer sequences used in qRT-PCR

Gene	Primer sequence (5′ to 3′)
LGALS1 (sense)	CTCCTGACGCTAAGAGCTTCG
LGALS1 (antisense)	CCAGGCTGGAAGGGAAAGAC
SOX5 (sense)	CCCTTGCATGTGAGTTTTCCC
SOX5 (antisense)	TGCCTTCTGAGGTGAGGTAGA
FGR (sense)	GGGCAGCAGACCACTATGG
FGR (antisense	GCCACTATCAAGGAAGCCAGG
CD11c (sense)	GGAGTGCCCAAGACAGGAG
CD11c (antisense)	GGAACTGGCTTATCACAGCTCT
OAS1 (sense)	GATCTCAGAAATACCCCAGCCA
OAS1 (antisense)	AGCTACCTCGGAAGCACCTT
FCRL4 (sense)	TCAGCTGGGAGAAGAAGAGGAA
FCRL4 (antisense)	GAGTTATCTGGGTGTTGTGTCTTTACC
FCRL4 (sense)	ATGGACCACATTCTTCAAAGGAG
FCRL4 (antisense)	CCCAGTAGTGCCGATGATACC
IL4R (sense)	CCGCCTCGTGGCTATAATAATC
IL4R (antisense)	GGCAGCCTTGTGAGGATCTT
TCL1A (sense)	GCTGCCCTTAACCATCGAGAT
TCL1A (antisense)	CAGCAGGCTTGGGCCTATC
EBNA 2 (sense)	TTAGAGAGTGGCTGCTACGCATT
EBNA 2 (antisense)	AGTGCTGGGTTACTGGCTAAGC

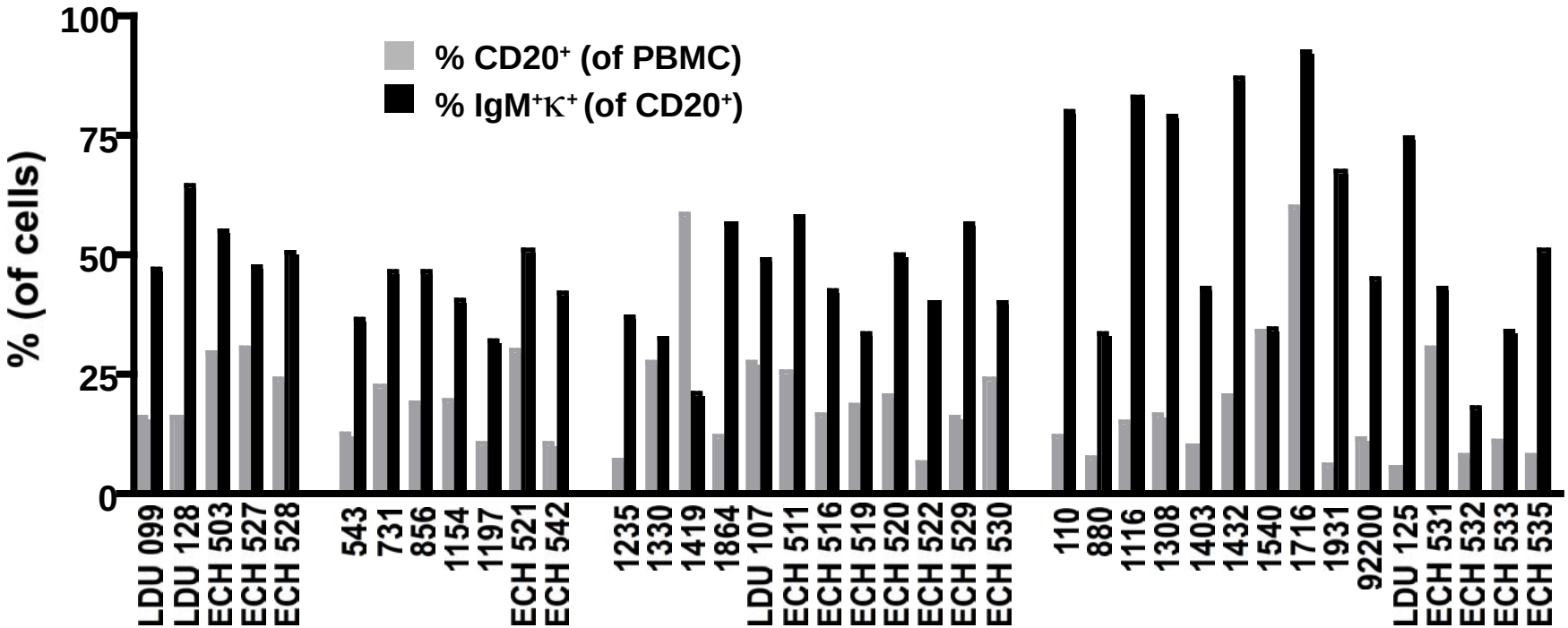

Figure S1. Percentages of $CD20^+$ and $IgM^+\kappa^+$ B cells among PBMCs from healthy individuals, sustained virologic responders, HCV^+MC^- patients, and HCV^+MC^+ patients. Gray bars represent percentages of $CD20^+$ PBMCs.
Black bars depict percentages of B cells that are $IgM^+\kappa^+$.

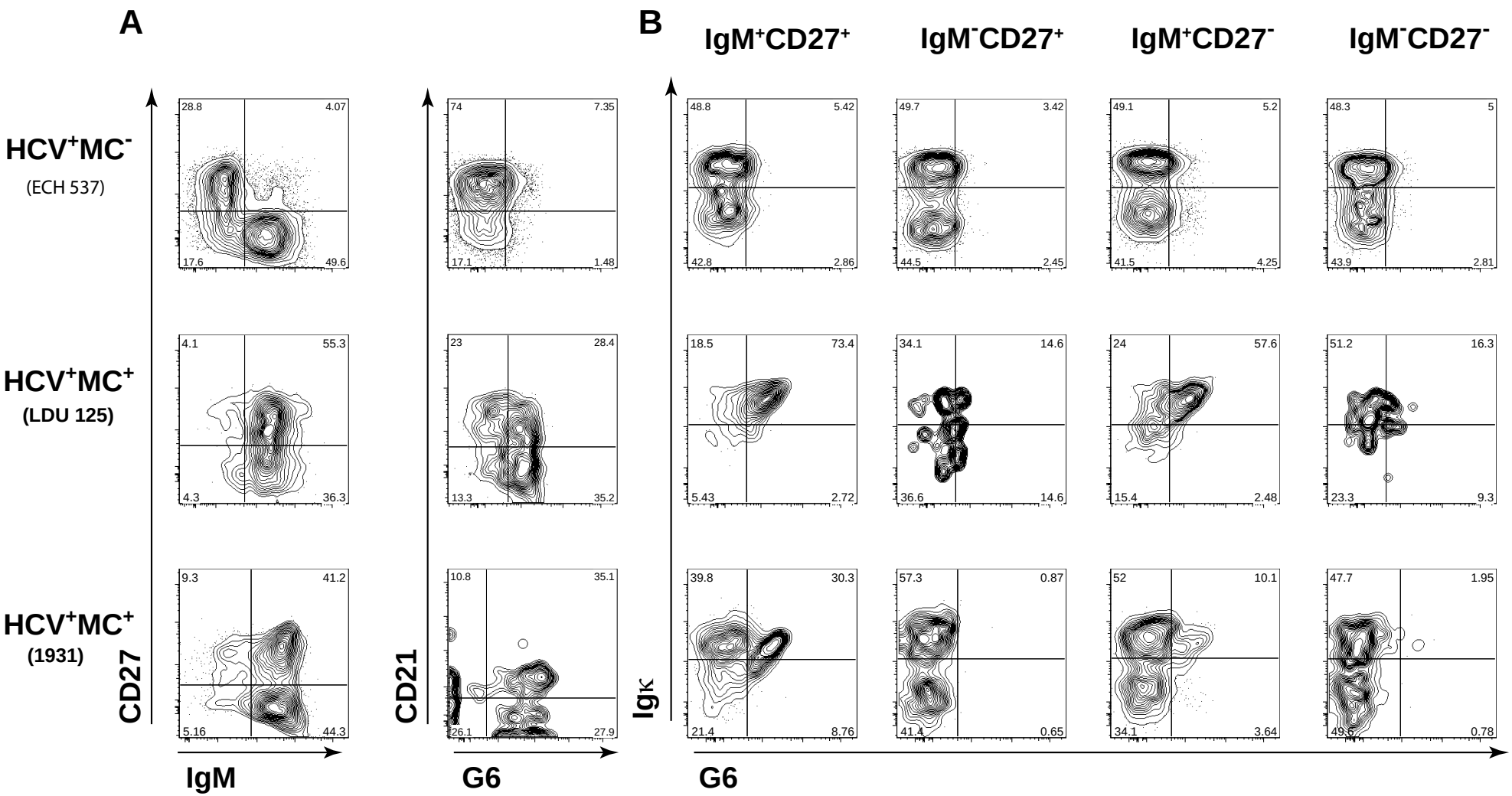

Figure S2. HCV^{+}MC^{+} patients' G6^{+} B cells have increased proportions of CD21^{low} and IgM$^{+}\kappa^{+}$CD27^{+} cells. B cell surface IgM, CD27, CD21 and G6 staining (A). Surface Igκ and G6 staining of IgM$^{+/-}$ CD27$^{+/-}$ B cell subsets (B). Analysis of CD20^{+} PBMCs from one HCV^{+}MC^{-} individual (ECH 537) and two MC^{+} patients (LDU 125 and 1931) are shown.

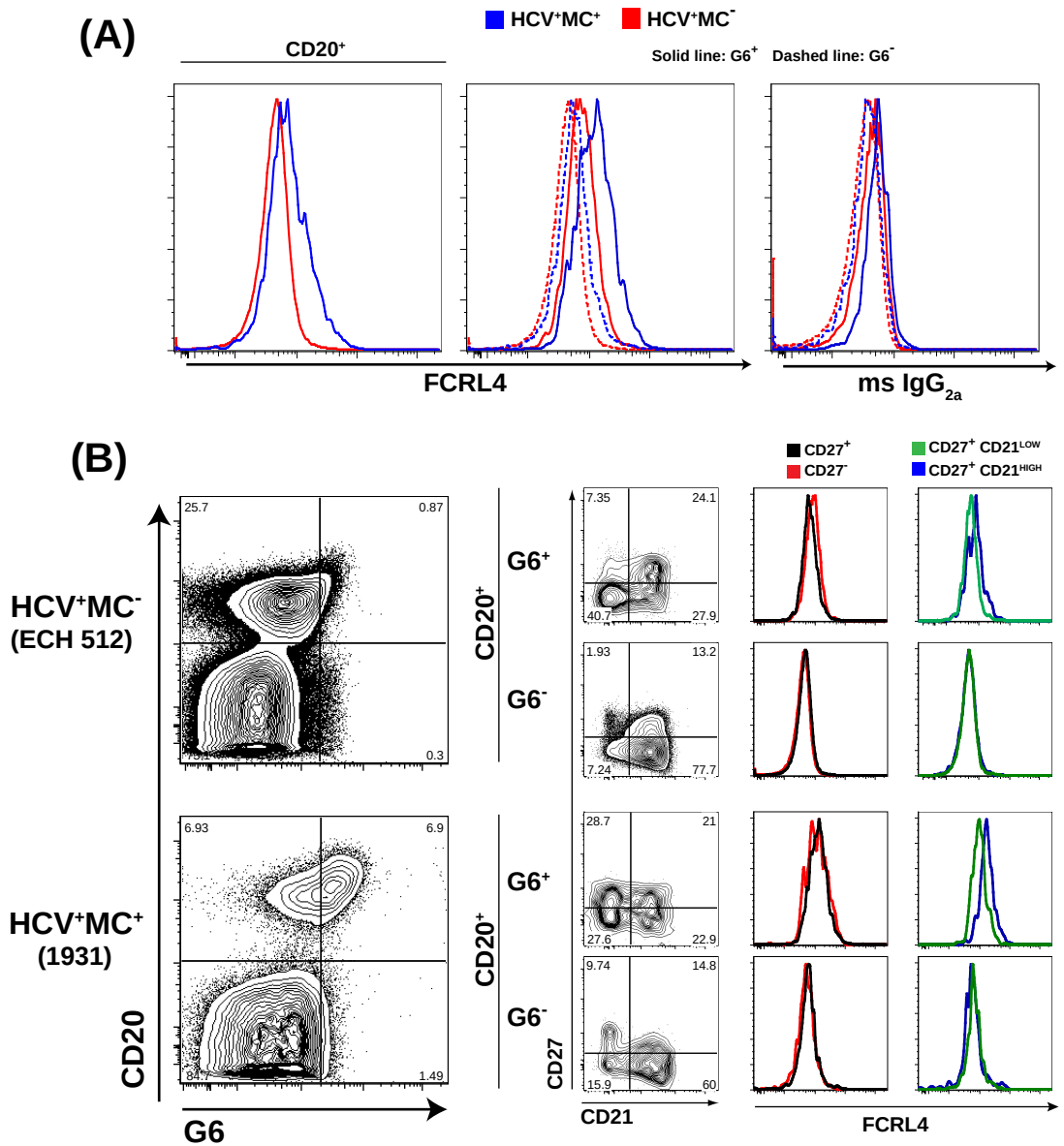

Figure S3. HCV$^+$MC$^+$ patients' G6$^+$ B cells have upregulated FCRL4 expression that does not significantly vary with CD27 or CD21 expression. Analyses of PBMCs from one representative one HCV$^+$MC$^-$ (ECH 512) and one HCV$^+$MC$^+$ patient (1931) (out of a total of six each) are shown. FCRL4 expression for total, G6$^+$, and G6$^-$ B cells. Mouse IgG2a isotype control is shown in the right panel (A). FCRL4 expression on CD27$^-$, CD27$^+$, CD27$^+$CD21^{low}, and CD27$^+$CD21^{high} G6$^+$ and G6$^-$ B cell subsets (B).

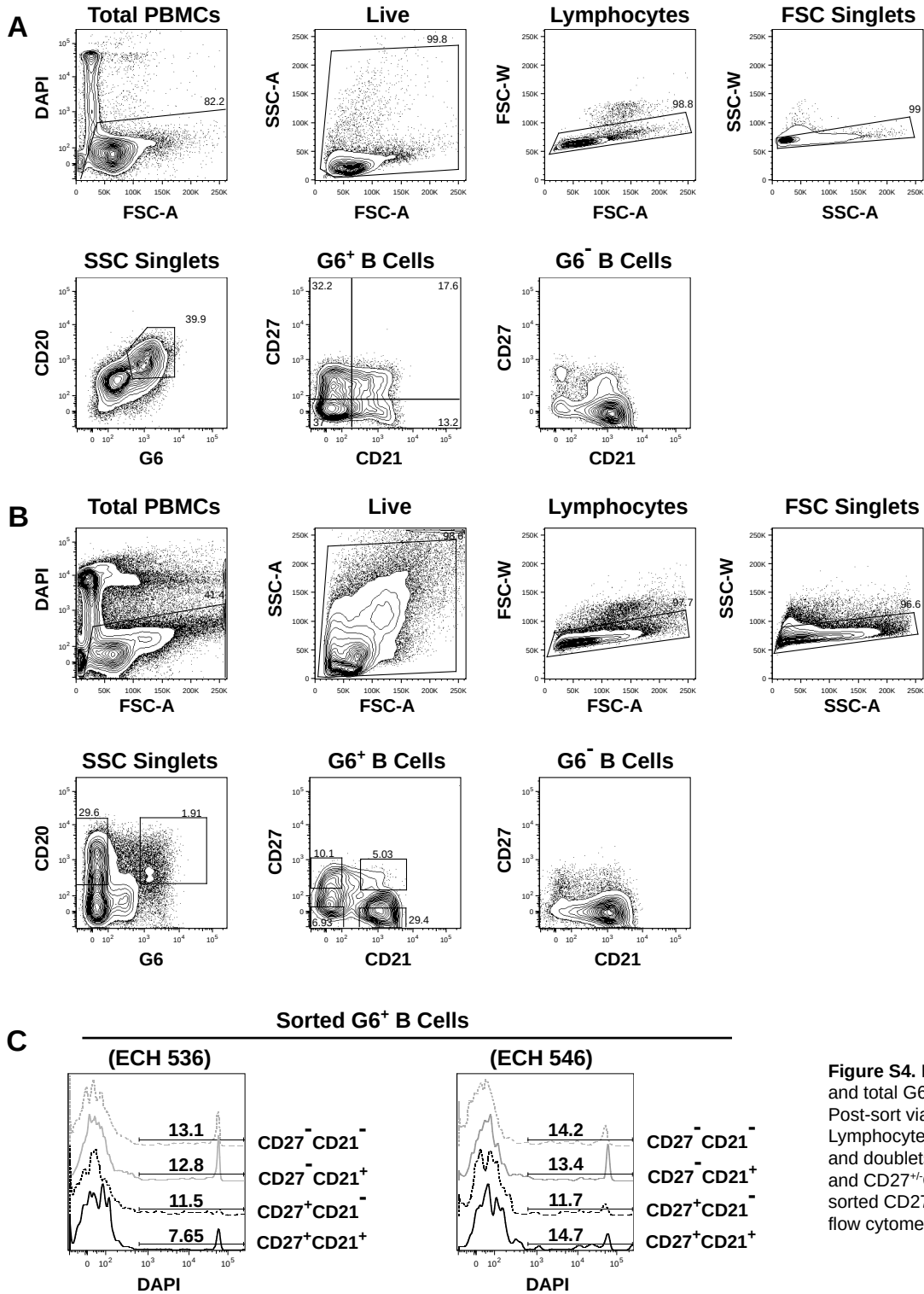

Figure S4. Bulk sorting strategy for isolation of $CD27^{+/-}CD21^{high/ow}$ and $CD27^{+/-}CD21^{high/low}$ $G6^{+}$ and total $G6^{-}$ B cell subsets from two HCV^{+} MC^{+} subjects, ECH 559 (A) and ECH 546 (B). Post-sort viability analyses of two samples, ECH 536 and ECH 546 are also depicted (C). Lymphocytes were identified by forward and side scatter characteristics, and $DAPI^{+}$ dead cells and doublets were excluded. $CD20^{+}$ $G6^{+}$ and $G6^{-}$ B cells were identified; $CD27^{+/-}CD21^{high/ow}$ and $CD27^{+/-}CD21^{high/low}$ $G6^{+}$ and total $G6^{-}$ B cells were bulk-sorted. For post-sort viability analyses, sorted $CD27^{+/-}CD21^{high/low}$ $G6^{+}$ B cell populations were re-stained with DAPI and re-analyzed by flow cytometry.